# - EFFICIENT LOW-ALLOY STEELS FOR HIGH PERFORMANCE STRUCTURAL APPLICATIONS

Ulf Engstrom*, David Milligan, Alex Klekovkin*
Sigurd Berg**
Bill Edwards***, Leonid Frayman***, Gerd Hinzmann***

*North American Höganäs, USA
** Höganäs AB, Sweden
***Hawk Precision Components Group, USA

## ABSTRACT

The demands on powder metal components for new automotive applications are placing more and more pressure on increased performance at reduced costs. This has created a demand for high performance and cost effective materials that can be used in a variety of applications. The growing interest for chromium as an alloying element for sintered steels is due to the excellent mechanical properties attainable both in the as sintered condition and after heat treatment, such as through hardening or case hardening. Among case hardening treatments, low pressure carburising is an attractive process aimed to improve fatigue strength and wear resistance of PM components.

In this paper properties achievable with a Cr-Mo pre-alloyed powder, Astaloy CrL, after processing by different conditions are described. Properties achieved at different density levels after conventional and high temperature sintering and low pressure carburising are compared. A case study of a production component is also described.

## INTRODUCTION

To continue to expand the P/M market into new applications cost effective materials with increased performance will be required. This can be achieved by different means. The development of new cost effective alloy systems, utilization of increased density by using new compaction techniques, sintering at higher temperatures and adoption of secondary heat treatments are all examples of means that either by themselves or in combination can be used to increase the material performance.

Pre-alloyed materials are one method of reaching higher performance levels. The most common alloying elements used in PM so far are nickel and molybdenum as these are not sensitive to oxidation during processing. Chromium is interesting as a alloying element due to its performance enhancing ability and relatively low cost. Chromium has not been utilized to a large extent in the past due to its high affinity to oxygen making it difficult to prevent from oxidation during sintering especially at lower sintering temperatures. However, with new pre-alloyed Cr containing powders in combination with the nitrogen-hydrogen atmospheres and furnaces available today, the advantages of chromium can be fully utilized [1-6].

Increased density level is another way to reach higher performance levels. By using higher compaction pressures, newly developed compaction technologies such as warm die and warm compaction densities up to 7.35 g/cm$^3$ can be obtained already after single compaction. By increasing the sintering temperature from conventional belt furnace sintering at 1120°C (2050°F) to 1270°C (2320°F) or more the performance of the material can be substantially improved.

Secondary heat treatments is another means to reach high performance levels. Although heat treatment is widely available, sintered Cr-Mo steels of densities up to 7.40 g/cm$^3$ are typically not suitable for heat treatment in conventional heat-treating furnaces. This is due to that at common heat treating temperatures 816-982°C (1500-1800$^0$F), the minimum oxygen partial pressure is too high to process sintered Cr-Mo steels without oxidation. Vacuum carburization is one way to overcome this and to achieve increased material properties.

The purpose of this paper is to investigate the performance levels achievable with a Cr-Mo pre-alloyed powder using different processing conditions in combination with vacuum carburization, quenching and tempering.

## EXPERIMENTAL PROCEDURE

### Powder/Materials

The material used in all experiments reported in this paper is based on a pre-alloyed Cr-Mo steel powder, Astaloy CrL™, from Höganäs AB, Sweden.
The chemical composition of this powder is shown in Table 1.

Table 1. Chemical composition of the base powder used

| Astaloy CrL™ | Cr, % | Mo, % | Fe, % |
|---|---|---|---|
| Content | 1.5 | 0.2 | Bal. |

Two premixes based on Astaloy CrL with the compositions listed in Table 2 were prepared. Asbury 1651 graphite was used in all cases and the nickel used was INCO 123. The lubricant used was Kenolube™ from Höganäs AB.

Table 2. Mix compositions

| Designation | Base Material | Graphite, $^w/_0$ | Ni, % | Lubricant, % |
|---|---|---|---|---|
| A | Astaloy CrL™ | 0.25 | - | 0.45 |
| B | Astaloy CrL™ | 0.25 | 0.70 | 0.45 |

### Experimental procedure

Transverse rupture strength, tensile strength and fatigue strength test specimens were compacted of each mix at North American Höganäs in a 100 ton hydraulic press. Different compaction pressures were used in order to obtain the target sintered densities of 7.05, 7.25 and 7.35 g/cm$^3$.

The test specimens were subsequently sintered at Hawk Precision Components Group in Falls Creek and Clearfield. Two different sintering furnaces and conditions were used. Conventional sintering at 1120°C (2050°F) was carried out in a 24 inch Abbott steel mesh belt furnace. For high temperature sintering at

1288°C (2350°F) an Abbot furnace with a silicone carbide belt was used. Table 3 details the sintering conditions used.

Table 3. Sintering conditions

| Description | Conventional sintering | High Temperature Sintering |
|---|---|---|
| Furnace type | Mesh belt | Silicone carbide belt |
| Temperature | $1120^0$C ($2050^0$F) | $1288^0$C ($2350^0$F) |
| Atmosphere | 95 $^v/_0N_2$ / 5 $^v/_0H_2$ | 95 $^v/_0N_2$ / 5 $^v/_0H_2$ |
| Time at Temperature | 30 minutes | 60 minutes |

Vacuum-carburizing was carried out in a furnace at Hayes Heat Treating Corp. Three different settings of the carburizing parameters were studied. As can be see from table 4 the differences between these were temperature, time, cooling media and carbon potential used. The reason to lower the temperature and shorten the time in setting 2 and 3 was to obtain a more well defined case than was obtained with setting 1 which resulted in an almost through hardened material. To study the effect of cooling media oil was used for setting 1and 2 and gas for setting 3. The carbon potential used in setting 2 and 3 was 1.02% compared to 1.37% for setting 1.

Table 4. Vacuum carburization parameters used.

| VC Parameters | Setting 1 | Setting 2 | Setting 3 |
|---|---|---|---|
| Temperature | 885°C ($1625^0$F) | 815°C ($1500^0$F) | 845°C (1550°F) |
| Vacuum Pressure | 100 torr | 100 torr | 100 torr |
| Carbon Potential | 1.37 %C | 0.93 %C | 1.02 %C |
| Carburizing time | 60 min | 10 min | 10 min |
| Diffusion time | 40 min | 5 min | 5 min |
| Quenching | Oil 32°C (90°F) | Oil 32°C (90°F) | Gas |
| Temper | $200^0$C ($395^0$F) 2 hours in air | $200^0$C ($395^0$F) 2 hours in air | $200^0$C ($395^0$F) 2 hours in air |

Transverse rupture strength, apparent hardness and dimensional change were determined for both materials after sintering and vacuum carburization with the parameters shown in setting 1. Tensile strength was also evaluated after this processing for material A. Transverse rupture strength was evaluated with specimens at a density of 7.25 g/cm$^3$ after vacuum carburizing with setting 2 and 3. Bending fatigue strength testing was limited to specimens with density 7.25 g/cm$^3$ and was carried out on vacuum carburized specimens using the parameters described by settings 2 and 3. Fatigue testing was carried out at Höganäs AB, Sweden, using a four point bending test machine with a load ratio of R= -1. Metallographic analysis was performed on material A and B after both sintering and vacuum carburization.

## RESULTS AND DISCUSSION

### Tensile strength

In figure 1 below the tensile strength obtained for material A after sintering at the two temperatures and vacuum carburizing with the parameters according to setting 1 is compared. By increasing the density from 7.05 to 7.35 g/cm³, the strength increase almost linearly. By increasing the sintering temperature from 1120°C to 1288°C (2050ºF to 2350ºF) the tensile strength is increased 15 to 20%. This is primarily due to more developed sintering necks, rounder pores, a change in microstructure and a slightly lower

oxygen content compared to what was achieved at the lower sintering temperature. As the material is shrinking slightly at the higher sintering temperature the density is also slightly increased which contributes to the improvement of the tensile strength. It is interesting to notice that the tensile strength obtained at the density level of 7.35 when sintered at 1120°C (2050°F) can be achieved at a density level of 7.05 g/cm³ when sintered at 1288°C (2350°F). It should be pointed out that considerable higher tensile strength after sintering could be achieved by increasing the carbon content, [1, 3], but in this study the objective has been to look at properties after carburization and for this purpose 0.25%C is relevant amount.

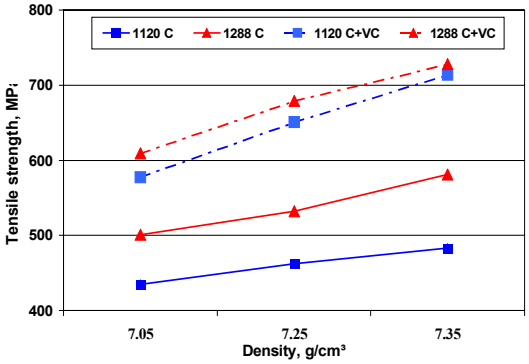


Figure 1. Tensile strength of material A after sintering and vacuum carburizing

A considerable increase of the tensile strength were obtained at both sintering conditions after vacuum carburization. The effect is particularly pronounced at the higher density levels. It can also be seen that the tensile strength obtained after vacuum carburization is about the same independently of the sintering temperature used. The tensile strength is increased about 40% for the material sintered at 1120°C (2050°F) and about 30 % for the material sintered at the higher temperature. The improvement is due to the formation of martensite in the surface.

**Transverse rupture strength (TRS)**

The transverse rupture strengths obtained for material A and B after processing at the different conditions are shown in table 5 below. As expected the transverse rupture strength increases with increased density for both material A and B. Material B achieved a slightly higher strength compared to material A when sintered at the lower temperature. By increasing the sintering temperature the transverse rupture strength increased about 5% for material A and about 10 to 15% for material B depending on the density. The higher strength levels obtained for material B is due to the addition of 0.7% nickel.

By vacuum carburizing the transverse rupture strength is increased 60 to 70 % for both material A and B when sintered at 1120°C (2050°F). By sintering at the higher temperature the increase is about 70% for material A and about 60% for material B. This increase is a result of the formation of a hard surface layer consisting of martensite in combination with a martensitic-bainitic core. Material B achieved about 5 to 10 % higher transverse rupture strength than material A at all conditions due to its higher alloying content.

Table 5. Transverse rupture strength of material A and B after different processing

| Sintering temperature, °C (°F) | Density, g/cm$^3$ | TRS, MPa (ksi) sintered | | TRS, MPa (ksi) vacuum carburized setting 1 | |
|---|---|---|---|---|---|
| | | Material | | Material | |
| | | A | B | A | B |
| 1120 (2050) | 7.05 | 917 (131) | 931 (133) | 1463 (209) | 1526 (218) |
| | 7.25 | 966 (138) | 1022 (146) | 1631 (233) | 1666 (238) |
| | 7.35 | 1022 (146) | 1099 (157) | 1680 (240) | 1736 (248) |
| 1288 (2350) | 7.05 | 945 (135) | 1008 (144) | 1568 (229) | 1666 (238) |
| | 7.25 | 1036 (148) | 1134 (162) | 1750 (250) | 1785 (255) |
| | 7.35 | 1085 (155) | 1246 (178) | 1841 (263) | 1904 (272) |

In table 6 the transverse rupture strength obtained after vacuum carburizing with the three different settings is shown for material A and B at a density of 7.25 g/cm$^3$. Material B achieved a slightly higher strength compared to material A for all three processing conditions. By increasing the sintering temperature the transverse rupture strength increased about 5 to 10% for both materials. The higher strength levels obtained for material B is due to the addition of 0.7% nickel. The strengths levels obtained with setting 3 are somewhat lower than those achieved with setting 2 which is due to the lower cooling rate obtained using gas as cooling media.

Table 6. Transverse rupture strength for material A and B after vacuum carburization **(**density 7.25g/cm$^3$**)**

| Sintering temperature, °C (°F) | Transverse rupture strength, MPa (ksi) | | | | | |
|---|---|---|---|---|---|---|
| | Vacuum carburization setting | | | | | |
| | 1 | | 2 | | 3 | |
| | Material | | Material | | Material | |
| | A | B | A | B | A | B |
| 1120 (2050) | 1631 (233) | 1666 (238) | 1498 (214) | 1526 (218) | 1415 (202) | 1442 (206) |
| 1288 (2350) | 1750 (250) | 1785 (255) | 1638 (234) | 1666 (238) | 1519 (217) | 1561 (223) |

**Apparent hardness**

The Rockwell apparent hardness achieved by the various processing techniques for material A and B are shown in table 7. The apparent hardness of the sintered materials are reported by HRB scale while the vacuum carburized materials were measured with the HRC scale. As can be seen the hardness increased with increased density for both materials at both sintering conditions, from 70 HRB to 83 HRB for material A. Material B achieved slightly higher hardness. By increasing the sintering temperature the hardness was slightly increased at all density levels for both materials. This is due to a change of the microstructure from upper bainite to lower bainite and due to slightly higher density obtained by the higher sintering temperature.

Table 7. Hardness, HRB and HRC, of material A and B after different processing

| Sintering temperature,°C(°F) | Density, g/cm$^3$ | Hardness, HRB Sintered | | Hardness, HRC Vacuum carburized | |
|---|---|---|---|---|---|
| | | Material | | Material | |
| | | A | B | A | B |
| 1120 (2050) | 7.05 | 70 | 78 | 36 | 36 |
| | 7.25 | 79 | 82 | 37 | 38 |
| | 7.35 | 82 | 85 | 39 | 39 |
| 1288 (2350) | 7.05 | 77 | 79 | 36 | 35 |
| | 7.25 | 81 | 84 | 38 | 36 |
| | 7.35 | 83 | 88 | 39 | 36 |

After vacuum carburization the apparent hardness increased dramatically at all densities and hardness in the range from 35 to 40 HRC were obtained after quenching and tempering for both materials independently of the sintering temperature used. That is due to the effect of changing the microstructure from upper bainite to martensite in the surface and slightly below the surface.

**Microhardness**

The micro hardness profiles obtained with TRS bars at a density of 7.25 g/cm$^3$ after vacuum carburization with settings 1,2 and 3 are shown in figure 2 below. As can be seen a less defined case was obtained when the parameters according to setting 1 were used. The micro hardness profile measured from the surface and inwards shows a more linear drop of the microhardness from 950 HV 0.1 in the surface to 650 HV0.1 in the center. A too high austeniting temperature in combination with a too long carburizing time and carbon potential can explain this result.

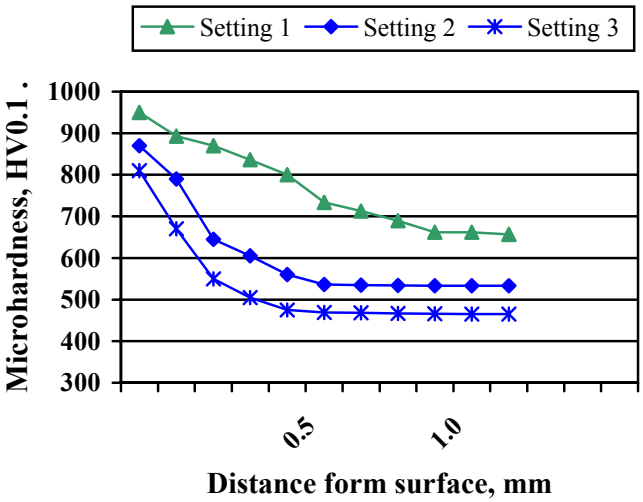


Figure 2. Micro hardness profiles obtained after vacuum carburization of material A with different parameters **(**density 7.25 g/cm$^3$**).**

The profile obtained with carburizing parameters according to setting 2 shows that a more defined case of about 0.4 mm was achieved. The surface hardness was about 900 HV0.1 while the core achieved a hardness of 550 HV0.1. This micro hardness profile is close to what is required in many gear applications.

The profile obtained with the parameters for setting 3 also shows that a defined case was obtained but the hardness levels are lower compared to what was achieved with setting 2. This is primarily due to the lower cooling rate obtained with the cooling gas media compared to the oil quench with setting 2.

**Fatigue strength**

Figure 2 and 3 below show the Wöhler diagrams achieved for material A after sintering at the two temperatures and vacuum carburizing using the parameters described for setting 2 in table 4 above. By comparing the results obtained for this material sintered at the lower temperature, figure 2, with the result obtained for the material sintered at the higher temperature, figure 3, it can be observed that the fatigue strength increased significantly, about 15%, from 368 MPa to 419 MPa.

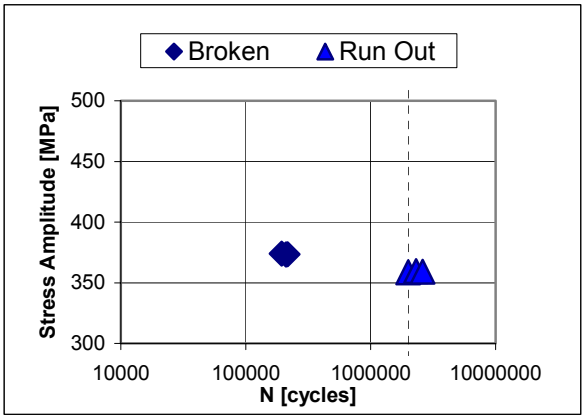


Fig. 2. Bending fatigue strength of vacuum carburized material A sintered at 1120°C (2050°F)

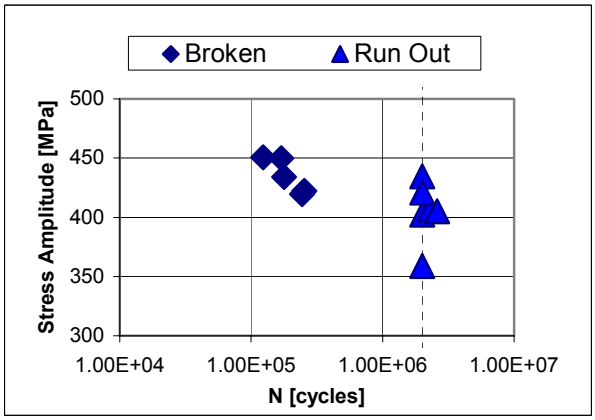


Fig. 3. Bending fatigue strength of vacuum carburized material A sintered at 1288°C (2350°F)

The benefit of the higher sintering temperature is related to rounder pores and improved sintering necks developed during sintering, and also due to improving of the microstructure from upper bainite and some ferrite to the lower bainite. This improves the mechanical properties in general and fatigue properties in particular.

In table 8 below the fatigue results obtained for both materials after vacuum carburization and quenching with oil and gas respectively are shown. The vacuum carburized material B achieved about 5% higher fatigue strength than material A when sintered at the lower temperature which is primarily due to the addition of 0.7% nickel. By increasing the sintering temperature the fatigue strength increased for both materials. However, at the higher temperature material A obtained the highest fatigue strength, 419 MPa compared to 401 MPa for material B. This might be due to a slightly different hardened case obtained for this material.

Table 8. Fatigue strength of material A and B after different processing

| Sintering temperature, °C (°F) | Density, g/cm$^3$ | Fatigue Strength, MPa (ksi) Material A | | Fatigue Strength, MPa (ksi) Material B | |
|---|---|---|---|---|---|
| | | Quenching media | | Quenching media | |
| | | oil | gas | oil | gas |
| 1120 (2050) | 7.25 | 366 (52) | 335 (48) | 386 (55) | 382 (55) |
| 1288 (2350) | 7.25 | 419 (60) | 342 (49) | 401 (57) | 385 (55) |

By utilizing gas quenching the fatigue strength obtained is lower for both materials compared to the oil quenched. This is primarily due to the lower cooling rate obtained with this media. Therefore the transformation to martensite in the surface layer is not as deep as in the oil quenched case which explains the lower fatigue strength levels. Material A shows a larger decrease compared to material B which might be explained by the lower hardenability of material A as it contains no nickel.

**Dimensional Change**

The dimensional change obtained after vacuum carburization was evaluated from die to as carburized size. Table 9 summarizes the dimensional change results for both materials.

Table 9. Dimensional change of material A and B after vacuum carburization

| Sintering temperature, °C (°F) | Density, g/cm$^3$ | Dimensional change, % vacuum carburized | |
|---|---|---|---|
| | | Material | |
| | | A | B |
| 1120 (2050) | 7.05 | 0.05 | -0.01 |
| | 7.25 | 0.07 | 0.04 |
| | 7.35 | 0.10 | 0.07 |
| 1288 (2350) | 7.05 | -0.17 | -0.23 |
| | 7.25 | -0.13 | -0.17 |
| | 7.35 | -0.07 | -0.12 |

As can be seen the dimensional change of both materials is depending on their density. When sintered at 1120°C (2050°F) both materials show a small growth. On the other hand when sintered at the higher temperature 2350ºF (1288°C) the two materials obtained a small shrinkage at all densities. Material B showed a slightly smaller growth at the lower sintering temperature and a slightly larger shrinkage at the higher temperature compared to material A. This is due to the addition of nickel which promotes shrinkage of the material during sintering.

**Unetched microstructure**

Figures 4 and 5 below show the pore structures obtained for material A at a density of 7.05 g/cm$^3$ density after sintering at 1120°C (2050ºF) and 1288°C (2350ºF) respectively.

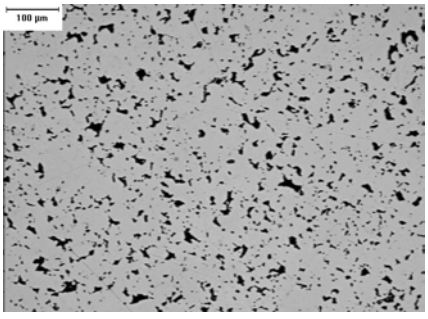


Fig. 4. Microstructure of material A sintered at 1120°C (2050°F).

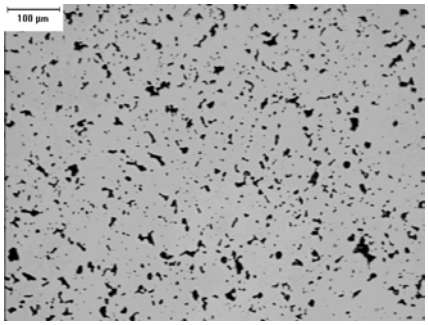


Fig. 5. Microstructure of material A sintered at 1288°C (2350°F).

As can be seen the utilization of higher sintering temperature improves the sintering necks and promotes pore rounding. The density has also increased slightly, about 0.03 g/cm³, due to the more active sintering resulting in a small shrinkage of the material.

**Etched microstructure**

The microstructures obtained for the two materials at a density of 7.05 g/cm³ are shown in figure 6 to 9 below. As can be observed from figure 6 the microstructure of material A sintered at conventional temperature 1120°C (2050°F) mostly consists of upper bainite and ferrite. This is related to the low carbon content and explains the relatively moderate level of tensile strength, transverse rupture strength and hardness obtained after sintering. On the other hand, high temperature sintering increase these properties which is mainly related to a change of the microstructure. As can be seen from figure 7 material A after high temperature sintering has a microstructure that consists of more upper bainite and less ferrite .

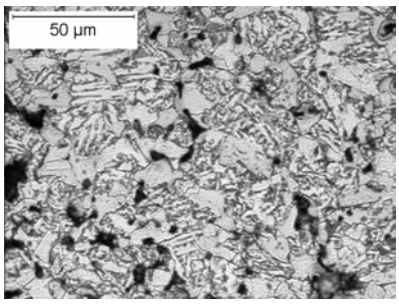


Fig. 6. Material A sintered at 1120°C (2050°F).

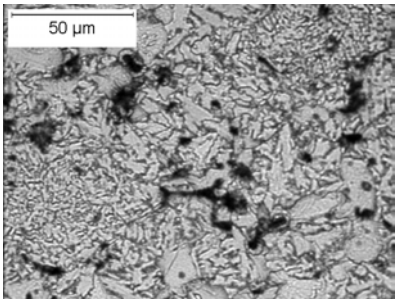


Fig. 7. Material A sintered at 1288°C (2350F).

The microstructure obtained for material B where 0.7% Ni has been was added consists of bainite, ferrite, Ni-reach austenite somewhere surrounded by martensite and some pearlite after sintering at the lower temperature, figure 8. At this sintering temperature Ni is not homogeneously distributed in the iron matrix and regions with higher nickel concentration appear as a white spots. By increasing the sintering temperature a microstructure consisting of more upper bainite, less ferrite with Ni-reach austenite surrounded by martensite was obtained, figure 9. The increased sintering temperature improves the homogenization rates nickel.

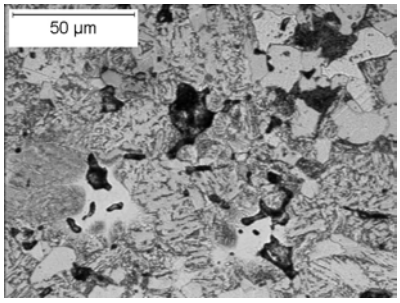


Fig. 8. Material B sintered at 1120°C (2050°F).

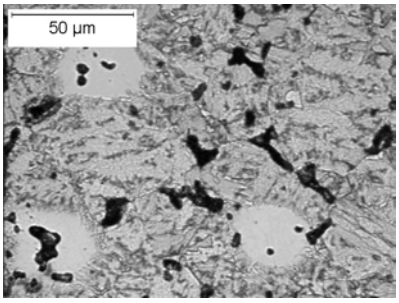


Fig. 9. Material B sintered at 1288°C (2350°F).

**Microstructures obtained after vacuum carburization**

The microstructures obtained after vacuum carburization with setting 1 are shown in figure 10 and 11 for both materials at a density of 7.25 g/cm$^3$ and sintered at the higher temperature. Material A obtained a high-carbon martensitic microstructure in the case (figures 10a, 10b) and high-carbon martensite with some-bainite in the center (figure 10c).

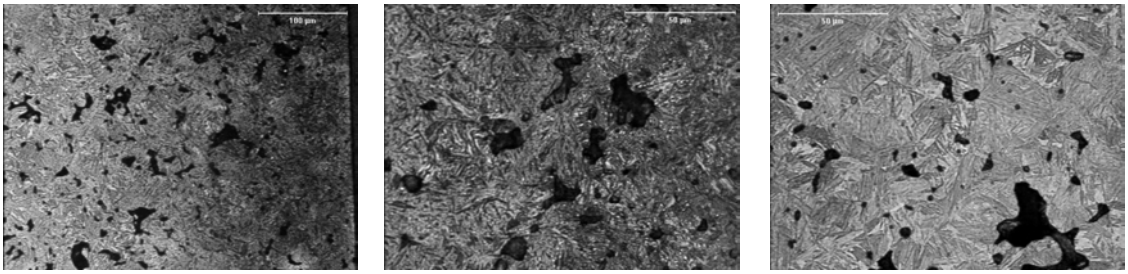

*a* *b* *c*

Figure 10. Material A, high-temperature sintered and vacuum carburized: *a* and *b* – surface, *c* – center.

Figure 11 shows that material B achieved a martensitic microstructure in the case (11a), and martensite with some bainite and Ni-reach martensite in the center (11b).

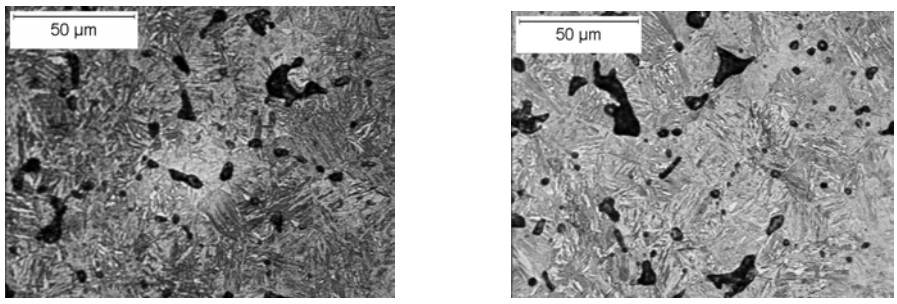


*a* *b*

Figure 11. Material B, high-temperature sintered and vacuum carburized: *a* – surface; *b* – center.

Figure 12a below shows that the vacuum carburized fatigue specimens quenched in oil (setting 2) achieved a surface layer consisting of high carbon martensite with some retained austenite. A minor amount of grain boundary carbides, cementite, could also be found to a depth of about 50 µm. The case depth obtained was about 0.3 mm. The core contained low-carbon martensite.

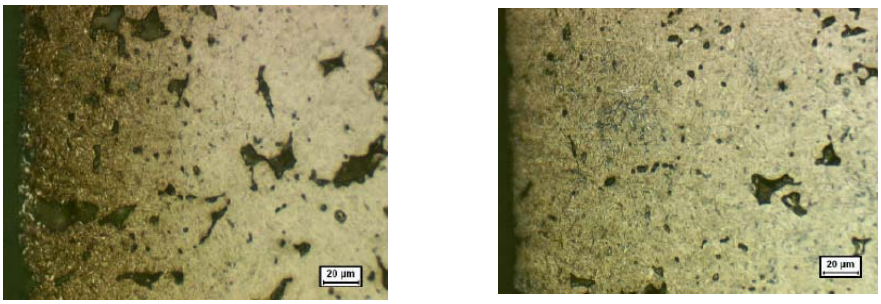


*a* *b*

Figure 12. Material A sintered at 1120°C (2050°F) and vacuum carburized:
*a* – oil quenched , *b* – gas quenched.

Due to the lower cooling rate the gas quenched material (figure 12b, setting 3) showed presence of martensite and lower bainite in the surface. The core has a microstructure consisting of very low carbon martensite, upper bainite and some ferrite. Some minor grain boundary carbides could also be found in the corner areas of the specimens.

The presence of a gradient in the microstructure in both materials with higher amount of martensite in the surface indicate, from the fatigue point of view, that beneficial compressive residual stresses have been induced in the surface.

The vacuum carburizing results obtained on the fatigue test specimens show that the case depth is too thin to get optimum bending fatigue performance for the test conditions. Un-notched fatigue specimens that have been used in this study should have a deeper case in order to be better adjusted to the stress profile. Theoretically a fully martensitic material with a carbon gradient that implies high carbon in the surface and low carbon in the core would be optimum. The expansion of martensite is depending on the carbon content, higher expansion for higher carbon, and beneficial residual compressive surface stress should be induced.

**CASE STUDY: VACUUM CARBURIZATION OF SPUR GEAR**

Many gears require a hard surface and a tough core and these features are commonly achieved by case hardening operations. Based on the results obtained with the test specimens reported previously it was decided also to study vacuum-carburization of spurs gear made of material A. The spur gear, shown in figure 13, had a 2-inch (50.8mm) diameter. The gears were compacted to a green density of 7.25 g/cm$^3$. Sintering was carried out at 1120°C (2050°F) and 1288°C (2350°F) respectively using the same equipment and conditions as described in table 3 above. Vacuum carburizing was carried out at Hayes Heat Treating Corp. in the same equipment used for the test bars. A picture of the equipment used is shown in figure 14.

Fig 13. Spur gear used for vacuum carburization.


Fig 14. Hayes vacuum carburization furnace.

The parameters used for vacuum carburization were the same as used with setting 2 described in table 4. After carburization dimensional change, micro hardness profiles and microstructures were determined.

## RESULTS

### Dimensional change

The dimensional change was evaluated by sampling 50 gears out of fifteen hundred gears of each processing condition. Table 10 shows the results obtained.

Table 10. Influence of sintering temperature and vacuum carburization on dimensional change of gears

| Sintering temperature, °C (°F) | Density, g/cm$^3$ | Dimensional change, % | |
|---|---|---|---|
| | | Sintered | Carburized |
| 1120 (2050) | 7.25 | 0.10 | 0.09 |
| 1288 (2350) | 7.25 | - 0.10 | - 0.16 |

As can be seen the gears sintered at 1120°C (2050°F) obtained a growth of 0.10% and a shrinkage of about the same when sintered at the higher temperature 1288°C (2350ºF). The dimensional change obtained during vacuum carburization followed by quenching in oil and tempering showed a slightly less growth compared to the sintered one in case of conventional sintering and a slightly larger shrinkage in case of high temperature sintering. As the dimensional change is related to the die size this means that the materials obtained a slight shrinkage during the vacuum carburization process. This shrinkage resulted in a slight density increase. These results are well in accordance with the results obtained with the test bars.

The scatter in the outer diameter was also calculated for the two different processed vacuum carburized gears. The results show (table 11) that the scatter is slightly higher for the gears sintered at the higher temperature compared to the scatter obtained when sintered at the lower temperature.

Table 11. Standard deviation of outer diameter on vacuum carburized gears

| Sintering temperature, °F (°C) | Standard deviation of outer diameter of gear |
|---|---|
| 1120 (2050) | 0.001 |
| 1288 (2350) | 0.002 |

However, the scatter is very low for both sintering conditions and this result show that parts can be sintered at high temperatures with similar control of the dimensional tolerances as is obtained by conventional sintering.

**Microhardness and microstructure**

The micro hardness and microstructure obtained in the surface and the core of a tooth of a high temperature sintered and vacuum carburized gear is shown in figure 15. The microhardness profile measured from the surface and inwards show that a case depth of about 0.4 mm had been obtained which is a common requirement for many gear applications. A micro hardness of 900 HV 0.1 has been achieved in the surface. The microstructure in the case is martensitic with small amount of retained austenite and a few carbides. In the core a softer martensite-bainite structure with lover carbon and ~35-40 % bainite has been formed.

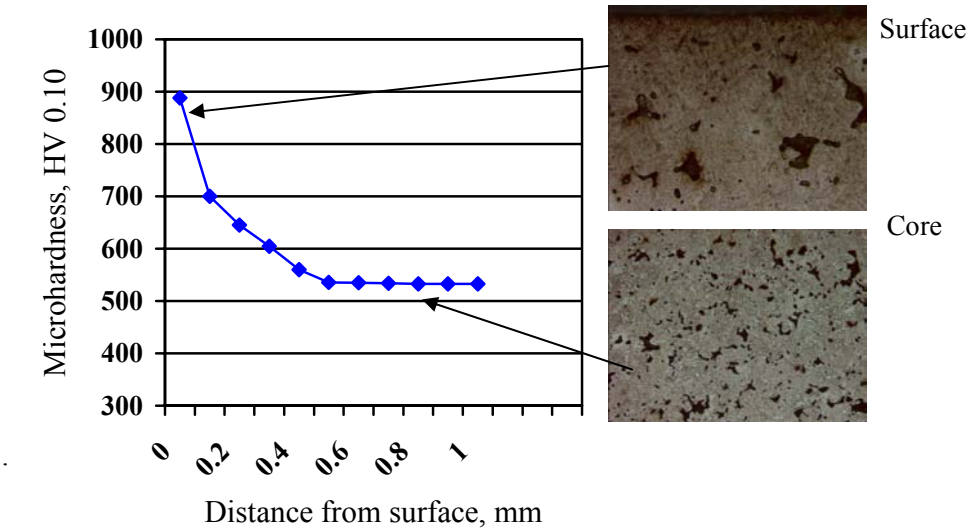


Fig. 15. Micro hardness and microstructure of vacuum carburized spur gear.

The results obtained with vacuum carburization on the gears corresponds very well with the results obtained with the test bars regarding both the microstructure and micro hardness profile both in the case and in the core. The data generated for test bars can therefore be used in the design of components like gears. However, it must be pointed out that depending on the component geometry and size the parameters used for vacuum carburization should be optimized to obtain the required case depth and micro hardness profile.

**CONCLUSIONS**

Vacuum carburization of materials based on Astaloy CrL$^{TM}$ significantly increases the mechanical properties compared to the as sintered material. The use of higher sintering temperature improve these properties further due to improved sintering necks, rounder pores, slightly higher density in combination with a change of the microstructure to lower bainite. By increasing the density these properties can be further increased. Depending on the processing conditions the transverse rupture strength can be increased 60-70%.

The bending fatigue strength of oil-quenched samples at a density of 7.25 g/cm$^3$ is in the range of 382 – 419 MPa depending on the sintering conditions. These levels are comparable to case hardened PM steels based on pre alloyed molybdenum powders.

Vacuum carburization has been demonstrated to be an effective process to case harden spur gears made of Astaloy CrL™ with carbon content in the range of 0.2 to 0.3 %. The data obtained with test bars and gears correspond very well and therefore data determined on test bars can be used in the design of gears that will be vacuum carburized.

**REFERENCES**


[1] S. Berg and B. Maroli, "Properties obtained by Chromium-Containing Material", PM2TEC 2002 World Congress On Powder Metallurgy & Particulate Materials in Orlando USA, 2002

[2] U. Engstrom, "Influence of sintering temperature on properties of low alloyed high strength PM materials", *Advances in Powder Metallurgy & Particulate Materials*, MPIF, 2001, part 7, pp.204~215

[3] I. Hauer, M. Larsson and U. Engstrom, "Properties of high strength PM materials obtained by different compaction methods in combination with high temperature sintering", *Advances in Powder Metallurgy & Particulate Materials*, MPIF, 2002, part 8, pp.29~37

[4] I. Nyberg, et al., "Effect of sintering time and cooling rate on sinterhardenable materials", *Advances in Powder Metallurgy & Particulate Materials*, MPIF, 2003, part 5, pp.101~110

[5] M. Larsson, S. Berg and B. Maroli, "Properties of Cr-alloyed PM materials", *European Powder Metallurgy Conference,* 2003

[6] O. Bergman, "Chromium-alloyed PM steels with excellent fatigue properties obtained by different process routes", *European Powder Metallurgy Conference,* 2003